

Assessment of American Bullfrog (*Lithobates catesbeianus*) spreading in the Republic of Korea using rule learning of elementary cellular automata

Gyujin Oh

Chonnam National University

Yunju Wi

Chonnam National University

Hee-Jin Kang

Chonnam National University

Seung-ju Cheon

Chonnam National University

Ha-Cheol Sung

Chonnam National University

Yena Kim

Hawaii Pacific University

Hong Sung Jin (✉ hjin@jnu.ac.kr)

Chonnam National University

Article

Keywords: Bullfrogs Spreading, Clustering, ECA, CNN, BOS, Habitat Suitability

Posted Date: November 8th, 2023

DOI: <https://doi.org/10.21203/rs.3.rs-3545672/v1>

License:   This work is licensed under a Creative Commons Attribution 4.0 International License.

[Read Full License](#)

Additional Declarations: No competing interests reported.

Assessment of American Bullfrog (*Lithobates catesbeianus*) spreading in the Republic of Korea using rule learning of elementary cellular automata

Abstract

The spread of American Bullfrog, one of the 100 of the World's Worst Invasive Alien Species, has a great impact on the surrounding ecosystem. Little is known about the tendency and pattern of how they are spreading in South Korea geographically. It is important to study the tendency of their spreading so that a proper mitigation can be applied when needed. This study is based on the results of national surveys that observed the distribution. The entire data is divided into 25 regional clusters using the divisive hierarchical clustering method. In order to estimate the degree of spreading, a sequence of spatial distribution is constructed for each cluster using the agglomerative clustering method. ECA(elementary cellular automata) is introduced to find rules governing the pattern variation in the sequence. Each cell represents either the observed or unobserved site of bullfrog. The number of Bullfrog Observed Site (BOS) in a sequence of each cluster is counted and used to define the spreading intensity. The rules of ECA are learned by the CNN(Convolution Neural Network) method and used to estimate and predict the spreading intensity by counting the expected number of BOS over 400 generations. Taking environmental factors into account, habitat suitability is used and obtained using Maxent. The spreading intensity is multiplied by the habitat suitability to get an assessment of bullfrogs spreading. The relative spreading assessment is estimated, which is classified into 4 groups; spreading intensively, spreading slowly, maintaining or declining population.

Keywords : Bullfrogs Spreading, Clustering, ECA, CNN, BOS, Habitat Suitability

Gyujin Oh¹, Yunju Wi¹, Hee-Jin Kang², Seung-ju Cheon², Ha-Cheol Sung³, Yena Kim⁴, Hong-Sung Jin^{1*}

¹ Department of Mathematics & Statistics, Chonnam National University, 77 Yongbongro, Bukgu, Gwangju 61186, Republic of Korea

² School of Biological of Sciences and Biotechnology, Chonnam National University, 77 Yongbongro, Bukgu, Gwangju 61186, Republic of Korea

³ Department of Biological Sciences, College of Natural Sciences, Chonnam National University, 77 Yongbongro, Bukgu, Gwangju 61186, Republic of Korea

⁴ Department of Mathematics, Hawaii Pacific University, 1 Aloha Tower Drive, Honolulu, HI 96813

* Corresponding author:

E-mail: hjin@jnu.ac.kr

Phone: +82 62 530 3346

37 **1 Introduction**

38 The American bullfrog, *Lithobates catesbeianus*, has been introduced to more than 40 countries
39 worldwide and is listed on the “100 of the World’s Worst Invasive Alien Species” (Database 2023).
40 American Bullfrog was introduced to Korea in 1957 and cultivated for the purpose of establishing new
41 food sources for human consumption, but due to its low economic efficiency and low demand as food,
42 most farm gave up on farming and released them into rivers illegally, and bullfrogs were spread all over
43 the country (Jang and Suh 2010; Kim 2009; Oh and Hong 2007). The spread of bullfrogs has a great
44 impact on the surrounding ecosystem such as increased competition with native species, predation and
45 the spread of ranavirus (Ficetola et al. 2010; Ficetola et al. 2007; Giovanelli et al. 2008; Groffen et al.
46 2019; Iñiguez and Morejón 2012; Kamoroff et al. 2020; Koo and Choe 2021; Nori et al. 2011; Park et
47 al. 2022; Schlaepfer et al. 2005). Bullfrogs have continued to spread in an environment without natural
48 enemies and have now spread nationwide except in some inland (mountain) areas in South Korea (Kang
49 et al. 2019; Koo and Choe 2021). The species was reported to occur at 2,716 sites, mainly along the
50 southern and western coasts, but was rarely distributed in the northern part of Korea or along the eastern
51 coast (Kang et al. 2019). It is also predicted that bullfrogs will continue to spread further in the future
52 (Koo and Choe 2021). Although several management strategies were implemented, the effectiveness of
53 the past control decisions is unclear (Chang et al. 2022). Meanwhile, some reports stated that local
54 natural enemies have appeared and are controlling the bullfrog population (No et al. 2017).

55 In this study, the likelihood of future spread is assessed by calculating the intensity of spread and habitat
56 suitability in 25 regions. Then they are classified into areas where the population is expected to continue
57 to increase, areas where there is no significant change in the current population, and finally areas where
58 the population is expected to decrease.

59 The study is based on the findings of national surveys including Natural Resources from 2006 to 2012,
60 the National Wetland Center Report from 2011 to 2017 and the National Institute of Ecology from 2015
61 to 2017 (Kang et al. 2019).

62 Since we do not have time series data of bullfrog distribution, we analyze the spatial distribution using
63 hierarchical divisive clustering method using scikit-learn 1.3.0 (da Silveira Vasconcelos et al. 2011;
64 Ermentrout and Edelstein-Keshet 1993; Patlolla 2018; Pedregosa et al. 2011). The entire data is
65 clustered into small clusters, and the degree of spreading is estimated by the evolution rules from the
66 elementary cellular automata scheme (Nagatani and Tainaka 2018; Wolfram 1983, 2002) in each small
67 cluster. CNN is trained to learn the evolution rules (Brodrick et al. 2019; Deneu et al. 2021; Duryea
68 2018; Kattenborn et al. 2021; Qin et al. 2020). By recognizing small clusters as a single image of 0’s
69 and 1’s, the number of 1’s is counted, which is the number of Bullfrog Observed Site (BOS). The ratio

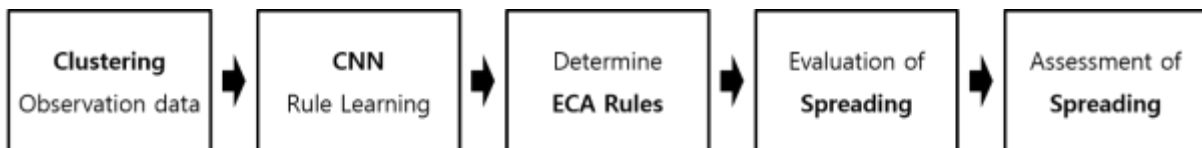
70 of the expected number of BOS at time t to the initial number of BOS is used to define the spreading
71 intensity. The estimated spreading intensity is multiplied by the habitat suitability to express the
72 assessment of bullfrog spreading by region. The habitat suitability is achieved using Maxent software
73 (Elith* et al. 2006; Ficetola et al. 2010; Ficetola et al. 2007; Steven J. Phillips 2017; Steven J Phillips
74 et al. 2017; Steven J Phillips et al. 2006; Steven J Phillips and Dudík 2008; Tesfamariam et al. 2022;
75 Venne and Currie 2021).

76

77 **2 Material and Methods**

78 Following the procedure shown in Fig. 1, several machine techniques are used such as clustering,
79 convolutional neural network, elementary cellular automata rule learning and Maxent to assess the
80 spreading intensity of bullfrogs by region.

81



82

83 **Figure 1.** The process to get an assessment of spreading. For each cluster, the agglomerative clustering method
84 is used to generate a clustering sequence, which is regarded as an image sequence, and the CNN method is applied
85 to learn ECA rules governing the sequence variation. For each ECA rule the number of 1's is counted, which is
86 the expected number of BOS to evaluate the intensity of spreading. Finally, the intensity is adjusted by multiplying
87 habitat suitability to get an assessment of spreading

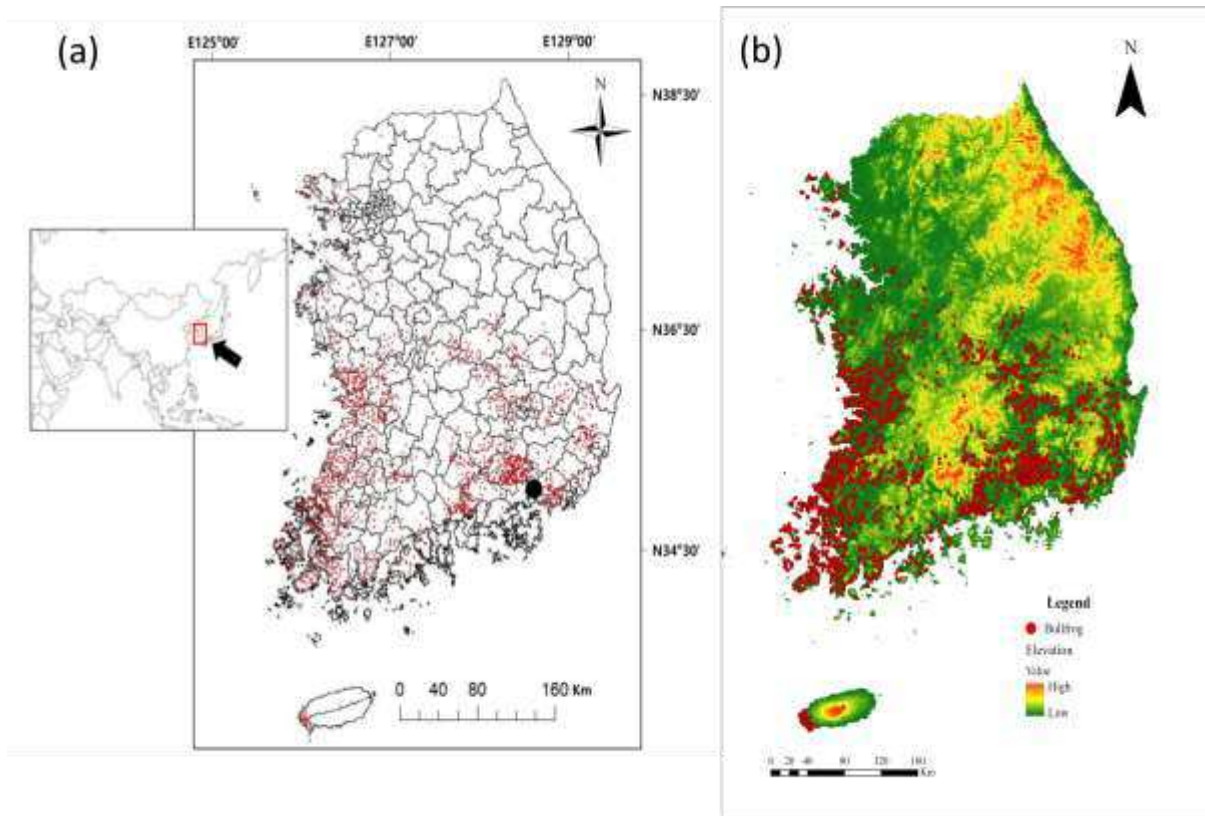
88

89 **2.1 Observation Data**

90 Data are collected from the results of several official nation-wide surveys, including the National Survey
91 of Natural Resources from 2006 to 2012, the National Wetland Center Report from 2011 to 2017 and
92 the National Institute of Ecology from 2015 to 2017 (Kang et al. 2019). Figure 2 shows the distribution
93 of American Bullfrog observed in South Korea. Time series data is not given.

94

95



96
 97 **Figure 2.** Distribution of bullfrog observations according to administrative districts and topography. The map
 98 above represents South Korea, and the data is between latitude $34^{\circ}58' - 36^{\circ}71'$ and longitude $126^{\circ}11' - 128^{\circ}2'$,
 99 covering approximately the southern half of South Korea. **a** It shows where bullfrogs have been found on the
 100 maps with the boundaries of administrative districts. **b** It shows where bullfrogs have been found on the
 101 topographic map. The highest elevations are red, then moving to orange, yellow, bright greens and finally dull
 102 greens at the lower elevations. It is mainly distributed in coastal wetlands or riverside wetlands and is rarely
 103 distributed in mountainous areas. This is a collection of findings over 60 years, with no temporal information

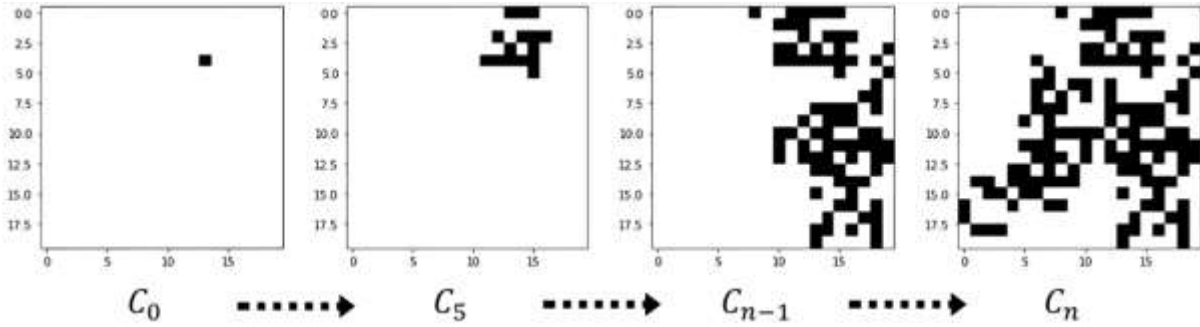
104

105 2.2 Clustering

106 In order to estimate the intensity of spreading by region, a sequence of spatial distribution from the
 107 observed data in Fig. 2 is constructed using the divisive hierarchical clustering method. All observations
 108 start in one cluster of full data, and splits are performed recursively as one moves down the hierarchy
 109 by grouping neighboring data into the same cluster (Patlolla 2018). The scikit-learn clustering software
 110 (Pedregosa et al. 2011) is used, and clusters are numbered according to the order in which they are
 111 formed. Clustering is performed until 25 clusters are formed to roughly match the size of the
 112 administrative district. Rectangular images consisting of 20 by 20 cells are created by uniformly
 113 dividing the latitude and longitude including all observations in each cluster. Latitude and longitude
 114 information for all clusters is in Table 1. If each cell had a bullfrog observation point, it is marked as 1,

115 otherwise it is marked as 0. Here, the point density of each cell is inhomogeneous. To estimate the
 116 spreading intensity of each cluster the agglomerate clustering method is performed in each cluster
 117 making the sequence of images, $C_0 \rightarrow C_1 \rightarrow \dots C_{n-1} \rightarrow C_n$. Figure 3 illustrates the agglomerate
 118 clustering steps, taking cluster #5 in Fig. 6d as an example.

119



120

121 **Figure 3.** Procedure of agglomerate clustering follows the sequence. The image sequence, $C_0 \rightarrow \dots C_5 \rightarrow$
 122 $\dots C_{n-1} \rightarrow C_n$, is created by applying the agglomerate clustering method to Cluster #5 in Fig. 6d. C_n corresponds
 123 to Cluster #5

124

125 2.3 Learning Elementary Cellular Automata Rules

126 ECA is introduced to find rules in the sequences for each cluster. ECA is a one-dimensional array of
 127 cells, where each cell takes either 1 or 0, representing BOS or not BOS, respectively. It generates next
 128 array depending on its own state and states of its two closest neighbors (Martinez et al. 2012; Weisstein
 129 2017; Wolfram 1983, 2002). Hence, 256 rules numbering from 0 to 255 are available to represent the
 130 sequence evolution. In this study only the even number rules are used. The odd number rules are
 131 excluded because it is making the next generation value 1 when both the current cell and the neighboring
 132 cells are 0, which is unsuitable for the biological spreading model. Each row in ECA represents one
 133 generation, where ECA is a one-dimensional array. The next generation is generated by the ECA rules.
 134 By reconstructing a one-dimensional array into a 2D image, each generation can be made of a sequence
 135 of images that change according to the ECA rules in Fig. 4.

136 The rules are learned by training the image change pattern using the Convolutional Neural
 137 Network(CNN) (LeCun et al. 2015; Webb 2018). CNNs are a subset of a class of deep learning
 138 algorithms, most commonly used for spatial pattern analysis in biology and ecology (Brodrick et al.
 139 2019; Kattenborn et al. 2021; Webb 2018). Additionally, CNN methods can efficiently classify the
 140 predicted distributions of many species (Deneu et al. 2021). In this simulation CNNs are trained with
 141 Keras package in TensorFlow (Martín et al. 2015).

142 **2.3.1 Generate training data**

143 The procedure is as follows:

- 144 • Create a 20 by 20 matrix by random seeding of 1's at 100, 200 and 300 initial points.
- 145 • Reshape the 20 by 20 matrix to a 1 by 400 matrix
- 146 • Generate the next generation of 1 by 400 matrix according to ECA rules.
- 147 • Reshape two consecutive 1D matrices to two consecutive 2D matrices, which are considered as one
- 148 sets of images, such as (C_{n-1}, C_n) in Fig. 3.
- 149 • Generate sets of image data for all 128 even rules
- 150 • Generate 500 sets of image data for each 100, 200 and 300 initial points for each rule

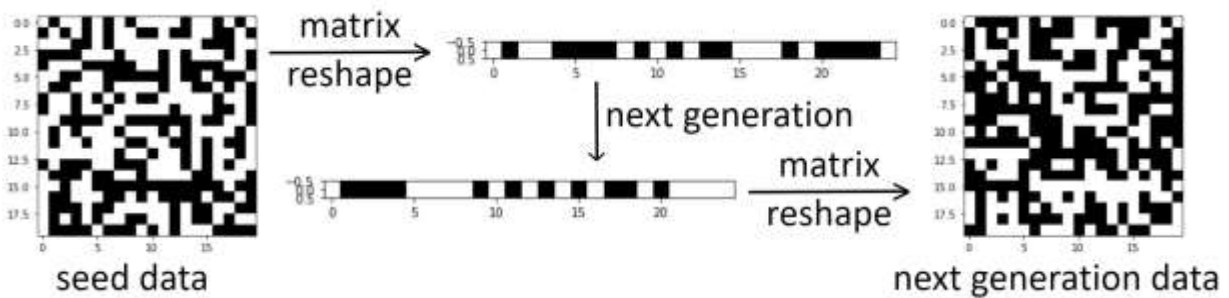
151 Hence, $500 \times 3 \times 128 = 192,000$ sets of image data are generated

152

153 **2.3.2 Training the rules**

- 154 • Separate 80% of training data and 20% of test data from total data
- 155 • Learning the rules using CNN(Convolution Neural Network) method (Fig. 4)

156



157

158 **Figure 4.** Seed 100, 200 and 300 random points on the 20 by 20 matrix. Reshape 20 by 20 matrix to 1 by 400
159 matrix, then apply the elementary cellular automata rules to make the new generation of 1 by 400 matrix. Reshape
160 the new matrix to 2 dimensional 20 by 20 matrix. To train the ECA rule learning, we generate 1500 number of
161 matrix pairs for all even rules of ECA by random seeding of 1's at 100, 200 and 300 initial points we generate

162

163 **2.4 Spreading Intensity**

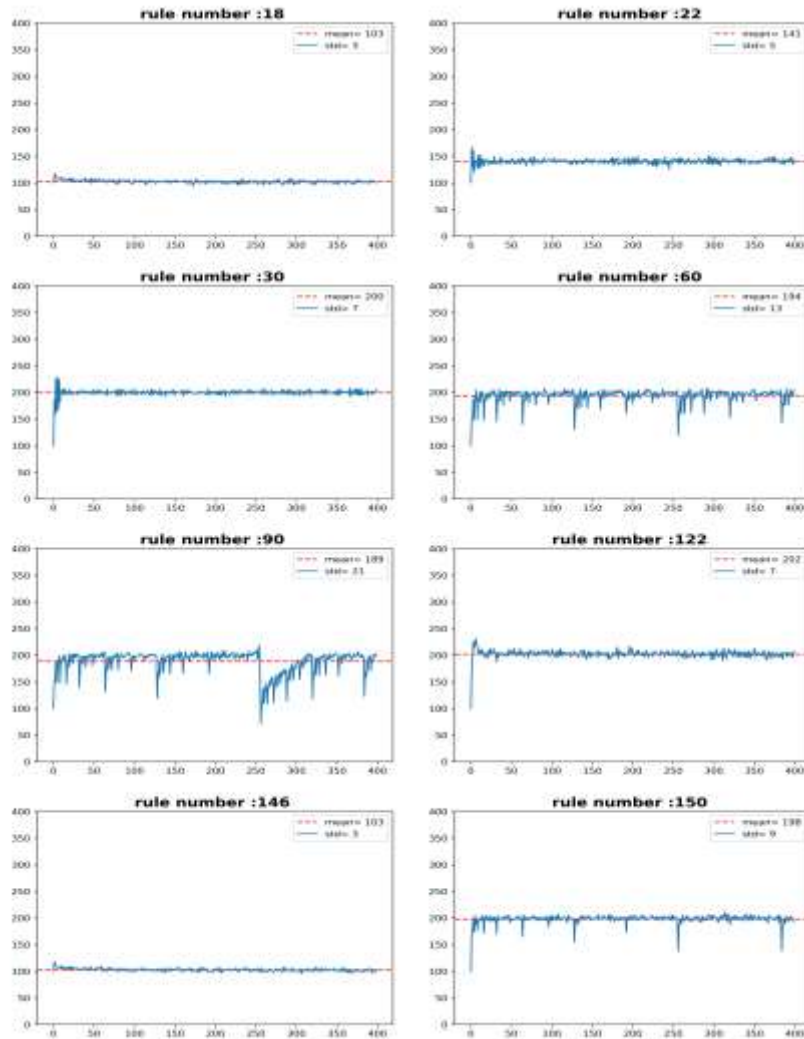
164 To estimate the intensity of spreading, the expected number of BOS variation depending on the rules
165 governing the evolution of clusters is estimated. As an initial value, a value of 1 is randomly given to
166 100 cells out of 400 cells of the image, then the number of 1's in the image is counted while evolving
167 over 400 generations according to all even-number rules of ECA. This procedure is repeated 10 times

168 to get the average number of 1's. Figure 5 shows the variaton in the expected number of BOS with the
 169 initial value set to 100 and the mean of each expected number of BOS for 400 generations for certain
 170 rules. The mean of the expected number of BOS divided by the initial value of 100 is defined as
 171 spreading intensity for each rule, which shows the growth rate of the expected number of BOS. The
 172 results for all even rules are in Table 3 in Appendix B.

173 The mean of the expected number of BOS according to each rule is multiplied by the percentile
 174 distribution of the rule to get the mean of the expected number of BOS of the cluster. Here the *spreading*
 175 *intensity* is defined as the mean of the number of BOS:

176
 177
 178
 179

$$\text{spreading intensity} = \sum_i \text{Percentile of rule } (x_i) * \text{mean of the expected number of BOS for rule } (x_i) / 100$$



180

181 **Figure 5.** Patterns of the expected number of BOS change by generation according to each rule. A value of 1
182 is randomly assigned to 100 cells out of 400 cells, and the number of cells having a value of 1 is counted up to
183 400 generations according to the ECA rule. It shows the variation in the expected number of BOS. Rules 18 and
184 146 show no significant change over 400 generations, and rules 30, 60, 90, 122, and 150 oscillate around the 200
185 BOSs, while rule 22 stays around 150 BOSs. The mean of the expected number of BOS is indicated in the legend
186 and shown in red dotted line.

187

188 **2.5 Assessment of spreading**

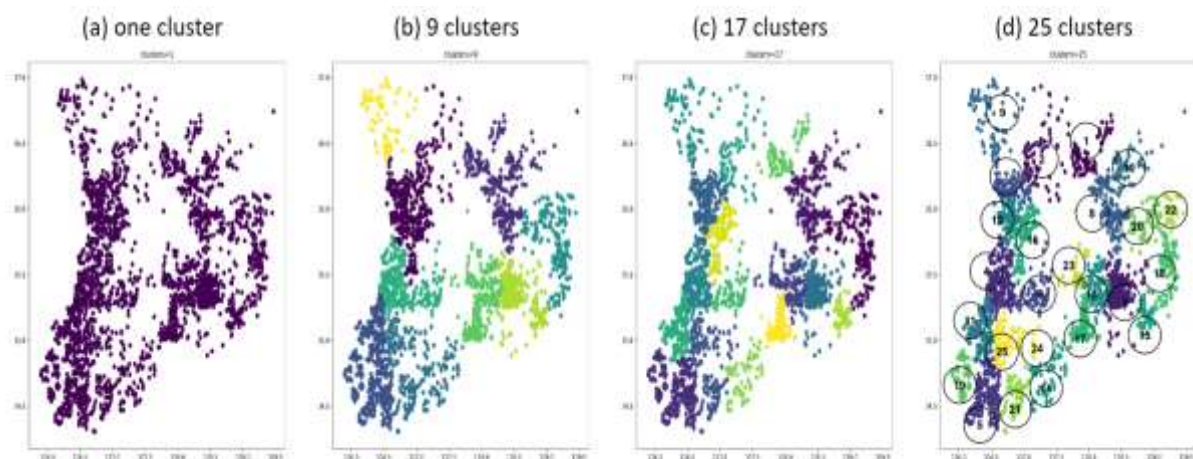
189 Since the spreading intensity is evaluated based on the mean of the expected number of BOS only
190 without considering any other environmental and biological variables, the final predicted spreading
191 intensity is weighted by the habitat suitability. The Maxent software (Maximum Entropy, version 3.4.1)
192 is used in estimating the relative habitat suitability of sites by comparing environmental conditions at
193 known observed sites to the available environmental conditions such as precipitation, temperature,
194 elevation and so on (Tesfamariam et al. 2022; Venne and Currie 2021). The main environmental factors
195 when using Maxent software are: annual mean temperature, mean diurnal range, temperature
196 seasonality, annual precipitation, precipitation of wettest month and precipitation of driest month.

197

198 **3 Simulation Results**

199

200 **3.1 Clustering**



201

202 **Figure 6.** Results of divisive clustering. **a** Observation data **b** divisive clustering after 9 clusters are
203 formed **c** divisive clustering after 17 clusters are formed **d** the size of the clusters became similar to the
204 size of the administrative district at 25 clusters are formed.

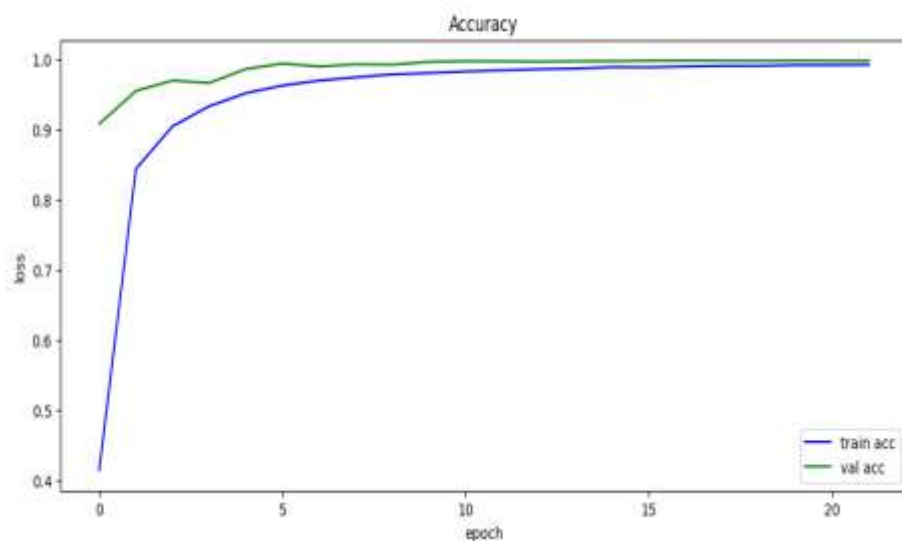
205

206 Using the hierarchical clustering method, the entire data is divided into 25 small clusters, and the size
207 of the clusters became similar to the size of the administrative district (Fig. 6d). The number of clusters
208 can be set to 1, 9 or 17, depending on the size of the region of interest (Fig. 6a-c). The common feature
209 of the clusters is the high density mainly around the waterside and wetland. However, the shape of the
210 cluster alone doesn't represent the spreading intensity for each cluster. Biological and environmental
211 informations are not taken into account when grouping the clusters

212 3.2 Learning the rules Using CNN

213 Figure 7 shows the accuracy of training the rules of ECA. The accuracy is more than 99%. This would
214 mean that the rule of changes in the bullfrog distribution could be learned with a very high confidence.

215



216

217 **Figure 7.** The accuracy of training. The x-axis (epoch) represents the number of training iterations, and the y-
218 axis (accuracy) represents the accuracy of the machine learning (the blue line (train acc; train accuracy) is the
219 accuracy curve of the training data. The green line (val acc; validate accuracy) represents is the accuracy curve
220 of the validation data). CNN is trained to learn ECA rules

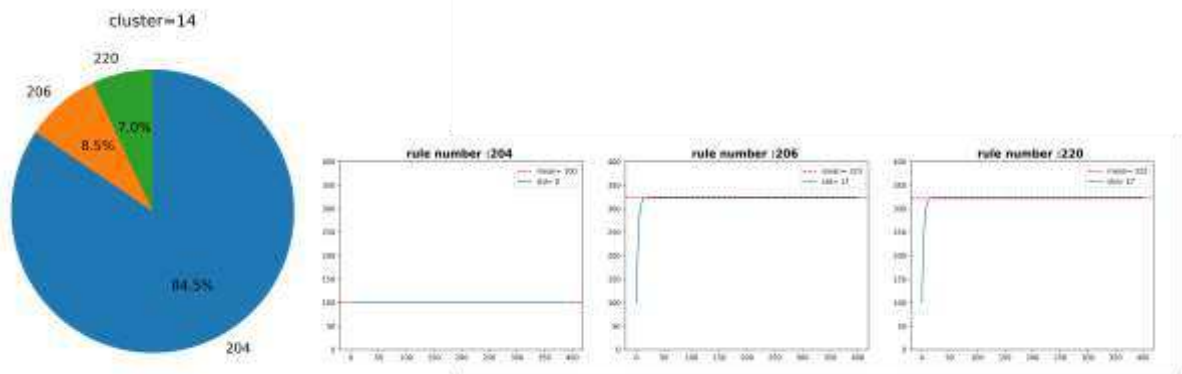
221

222 3.3 Spreading intensity

223 Figure 8 in Appendix A shows the distribution of rules predicted through CNN learning for each cluster
224 in Fig. 6d. The expected number of BOS for all 128 ECA rules estimated over 400 generations are in
225 Table 3 in Appendix B. For cluster 14 as an example, it shows a distribution of 84.5% for rule 204, 8.5%
226 for 206, and 7.0% for rule 220 in Fig. 9. The mean of the convergent number for rule 204 is 100, for
227 the rule 206 is 323, and for the rule 220 is 322. Therefore, if bullfrogs are found in 100 cells now, the

228 expected number of converged BOS in cluster 14 can be calculated as
 229 $1.00*0.845+3.23*0.085+3.22*0.07=1.34495$, which is the spreading intensity for the cluster 14. The
 230 spreading intensity of all clusters are shown in Table 1

231



232

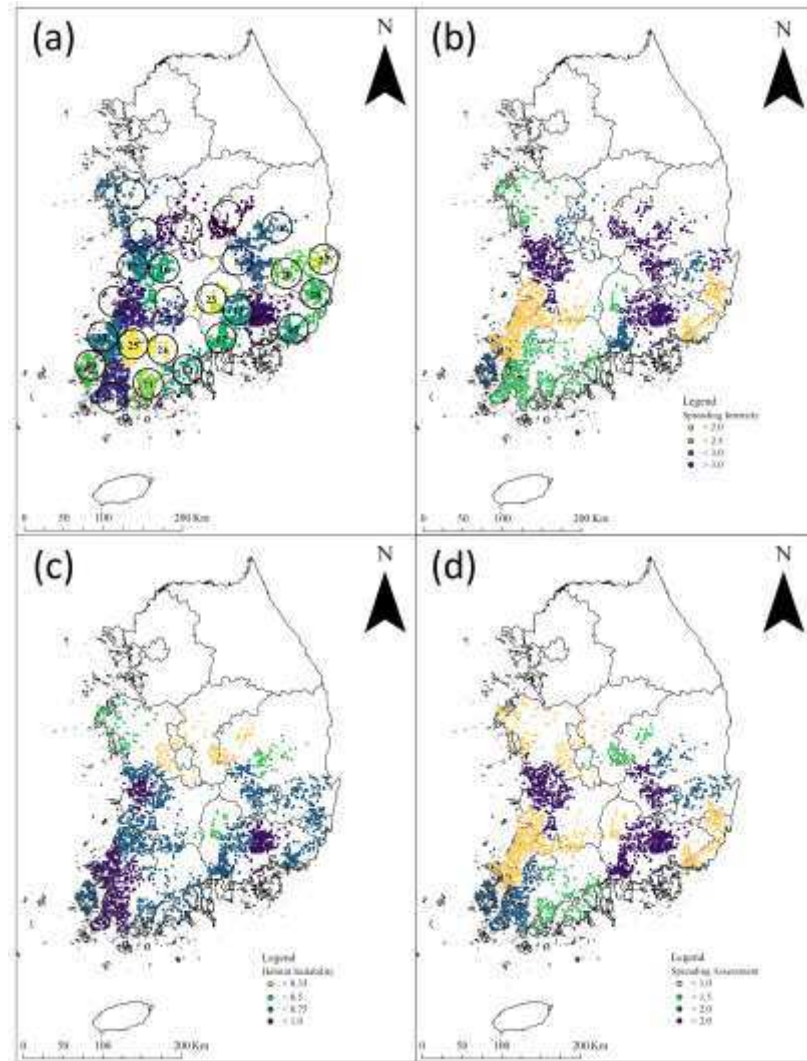
233 **Figure 9.** Distribution of rules for cluster 14. It consists of rules 204, 206, and 220 corresponding to 84.5%,
 234 8.5%, and 7.0% respectively. The mean of the convergent number of BOS for rule 204 is 100, for the rule 206 is
 235 323, and for the rule 220 is 322

236

237 3.4 Spreading Assessment

238 Figure 10 shows the Spreading Intensity (SI), Habitat Suitability (HS) and Spreading Assessment (SA)
 239 of 25 clusters. Figure 10b shows the SI distribution. It does not reflect environmental and biological
 240 variables, and it shows the spreading intensity calculated only by machine learning methods (clustering,
 241 CNN, etc.). Areas that are already saturated may have low SI values, and areas with low saturation,
 242 such as mountainous areas, may have large SI values. Figure 10c represents HS distributions. HS values
 243 obtained by using Maxent software reflect ecological environmental factors for the bullfrogs. Figure
 244 10d shows the distribution of SA values obtained by multiplying SI values and HS values. The HS value
 245 ranges from 0 to 1, and the closer it is to 1, the more suitable. All distribution values are relative and
 246 expressed in four stages: strong spreading, weak spreading, strong retention, and weak retention.

247



248

249 **Figure 10.** Results of 25 clusters. **a** 25 Clusters : Divisive clustering is performed until the clustering became
 250 similar to the local administrative districts. **b** Spreading Intensity(SI): It does not show a strong spreading intensity
 251 in coastal and wetland areas. This suggests the possibility that spreading has already occurred to saturation. **c**
 252 Habitat Suitability(HS): Habitat suitability calculated using Maxent software. If the SI, the spreading intensity, is
 253 weak at a high HS, it means that spreading has already occurred sufficiently. **d** Spreading Assessment(SA): Areas
 254 with high probability of spreading are marked with red dots

255

256 Table 1 shows the result of calculating the spreading assessment. From left to right, each column
 257 represents the number of BOS per cluster, spreading intensity, habitat suitability, spreading assesment,
 258 and geometric center latitude and longitude. The higher the value, the greater the probability of
 259 spreading. SI is a value obtained through machine learning using only BOS data. Environmental and
 260 biological factors were reflected through Habitat Suitability (HS) to get Spreading Assessment (SA).

261 **Table 1** The results of bullfrog spreading for 25 clusters

Clustering Number	number of BOS	SI	HS	SA	Longitude	Latitude
1	77	3.25	0.331892778	1.078651528	127.99	36.42
2	83	2.87	0.336620682	0.966101357	127.27	36.42
3	267	3.1	0.772864513	2.395879991	128.47	35.36
4	202	1	0.740367631	0.740367631	126.64	35.47
5	168	2.48	0.794083093	1.96932607	126.43	34.58
6	103	1.51	0.594828446	0.898190953	127.2	35.36
7	127	3.25	0.713751758	2.319693214	126.77	36.16
8	125	3.24	0.65006152	2.106199325	128.33	36
9	96	2.08	0.460205108	0.957226626	126.47	36.71
10	58	3.46	0.473968133	1.639929741	128.6	36.33
11	205	1.26	0.791182732	0.996890243	126.46	35.08
12	135	3.25	0.781342992	2.539364724	126.76	35.93
13	98	3.42	0.62174352	2.12636284	128.14	35.4
14	68	2.23	0.634174926	1.414210085	127.36	34.73
15	87	1.35	0.690117529	0.931658665	128.88	35.18
16	113	3.16	0.673967381	2.129736922	127.01	35.78
17	136	2.91	0.701436489	2.041180182	127.91	35.11
18	107	1.1	0.62500829	0.687509118	129.21	35.57
19	70	2.66	0.697356021	1.854967015	126.11	34.73
20	65	2.86	0.6193504	1.771342144	128.88	35.89
21	58	2.14	0.617724528	1.321930491	126.88	34.58
22	30	3.33	0.573416667	1.9094775	129.28	35.99
23	37	2.02	0.3649146	0.737127492	127.81	35.53
24	37	2.21	0.575529162	1.271919448	127.03	34.99
25	65	2.22	0.804474672	1.785933772	126.66	34.98

262

263 The final spreading assessment is the spreading intensity multiplied by the habitat suitability estimated
 264 by Maxent software 3.4.1. The higher the value, the greater the probability of spreading. Table 2 shows
 265 relative spreading assessments. Four cluster groups are created based on assessment scores. The clusters
 266 in groups (I) and (II) show spreading assessment scores greater than 2, which means that they will
 267 continue to spread. Clusters in group (III) show the scores of 1 to 1.5, which can be considered as slow

268 spreading or maintaining the population. For group (IV) clusters, the spread appears to have stopped,
 269 and the population may decline, especially in clusters #4, #8, and #23

270

271 **Table 2** Groups of Spreading Assessment

Group	Spreading Assessment (SA)	Cluster Number(#)	Relative Results
Group (I)	$2.0 < SA$	3,7,8,12,13,16,17	Continue to spread intensively
Group (II)	$1.5 < SA < 2.0$	5,10,19,20,22,25	Continue to spread
Group (III)	$1 < SA < 1.5$	1,14,21,24	maintain population
Group (IV)	$SA < 1$	2,4,6,9,11,15,18,23	maintain population and possibly decrease in 4,18,23

272

273 **4 Discussion**

274 Clustering is performed until 25 clusters are formed to roughly match the size of administrative districts.
 275 If the stopping number of clusters is changed in this method, the target range and the convergence of
 276 the expected number of BOS may also change, so the number of clusters should be adjusted to properly
 277 include the region of interest.

278 In this study, the `numpy.reshape()` function (Harris et al. 2020) was used to rearrange two-dimensional
 279 images into one-dimensional array. Another future study is needed to apply ECA according to various
 280 array arrangements. When applying the ECA rules, zero padding was applied to both end points, that is,
 281 0 is used for the -1^{th} and 401^{st} virtual cells. It is assumed that Bullfrog has been never found outside the
 282 cluster. If found, they should be included in other clusters.

283 Since the agglomerate clustering method is used in generating image sequences to train convolutional
 284 neural network, rules for increasing the expected number of BOS were mainly distributed as shown in
 285 Fig. 8 in Appendix A. However in some rules the expected number of BOS appeared to increase rapidly
 286 at first show various patterns, such as converging to a certain value (e.g. rule 124) or decreasing over
 287 time (e.g. rule 120) in Table 3 in Appendix B.

288 In estimating spreading intensity, the mean of the expected number of BOS is used, but the slope can
 289 be more useful in expressing the tendency of spreading as shown in Table 3 in Appendix B. Further
 290 research is needed to define the appropriate diffusion strength according to the convergence pattern of
 291 the expected number of BOS.

292 Since the spreading intensity is estimated based only on the data currently found it is relatively low in
293 the region where spreading is already completed. Low spreading intensity may mean that it is already
294 saturated, which is different from extinction. Alternatively, the carrying capacity may decrease from a
295 population dynamics perspective due to the emergence of natural enemies or human quarantine.

296 The size of cells is identical in each cluster. The density of observations in a cell is uniformly 0 or 1,
297 where 1 being BOS. However, in each cell, the number of bullfrog observations are different. Hence,
298 the cloglog(default in Maxent 3.4.1) option is used to treat occurrence records as points rather than grid
299 cells to estimate relative habitat suitability (Steven J Phillips et al. 2017).

300 Geographical characteristics and ecological characteristics are replaced by habitat suitability using
301 Maxent but more detailed cultural characteristics should be applied. In addition to observations,
302 appropriate detection methods for bullfrogs, such as eDNA methods or audio recording devices, are
303 required (Kamoroff et al. 2020).

304 Only the accuracy of machine learning is presented as a verification method. In order to verify its
305 validity, it is necessary to select 3 or 4 regions and observe the spreading intensity continuously for
306 several years to generate time series data and compare it with the expected values from simulations.

307

308 **5 Conclusion**

309 In this paper, the relative spreading assessment is estimated for South Korea using machine learning
310 methods. The extent to which bullfrogs continue to spread at observation sites is quantified and assessed.

311 Since there is no time series data, the accumulated data are used to evaluate the spread of bullfrogs by
312 creating a spatial series using machine learning. In this process, biological and environmental factors
313 were not considered at all. Habitat suitability obtained by using Maxent software includes
314 environmental and biological factors, which were applied in the form of weights to the final spread
315 classification evaluation

316 The cell where bullfrogs are found (BOS: bullfrog observed site) is assigned to 1, and the number of
317 1's in 400 cells composed of 1's and 0's is counted and used as the spreading index of bullfrogs. The
318 mean of the number of BOS divided by the initial value of 100 is assumed as a measure of spreading
319 intensity for each rule. The spreading intensity is weighted by the percentile of the rules estimated by
320 the CNN method. Spreading assessment is the spreading intensity multiplied by the habitat suitability,
321 which can be used as one of the index showing the tendency of spreading.

322 **Acknowledgements** This work was supported by Korea Environment Industry & Technology
323 Institute(KEITI) through Exotic Invasive Species Management Program, funded by Korea Ministry of
324 Environment(MOE)(2018002270001). Additional funding was provided by the National Research
325 Foundation of Korea (NRF), which is funded by the Ministry of Education, Republic of Korea (NRF-
326 2020R1I1A3071769).

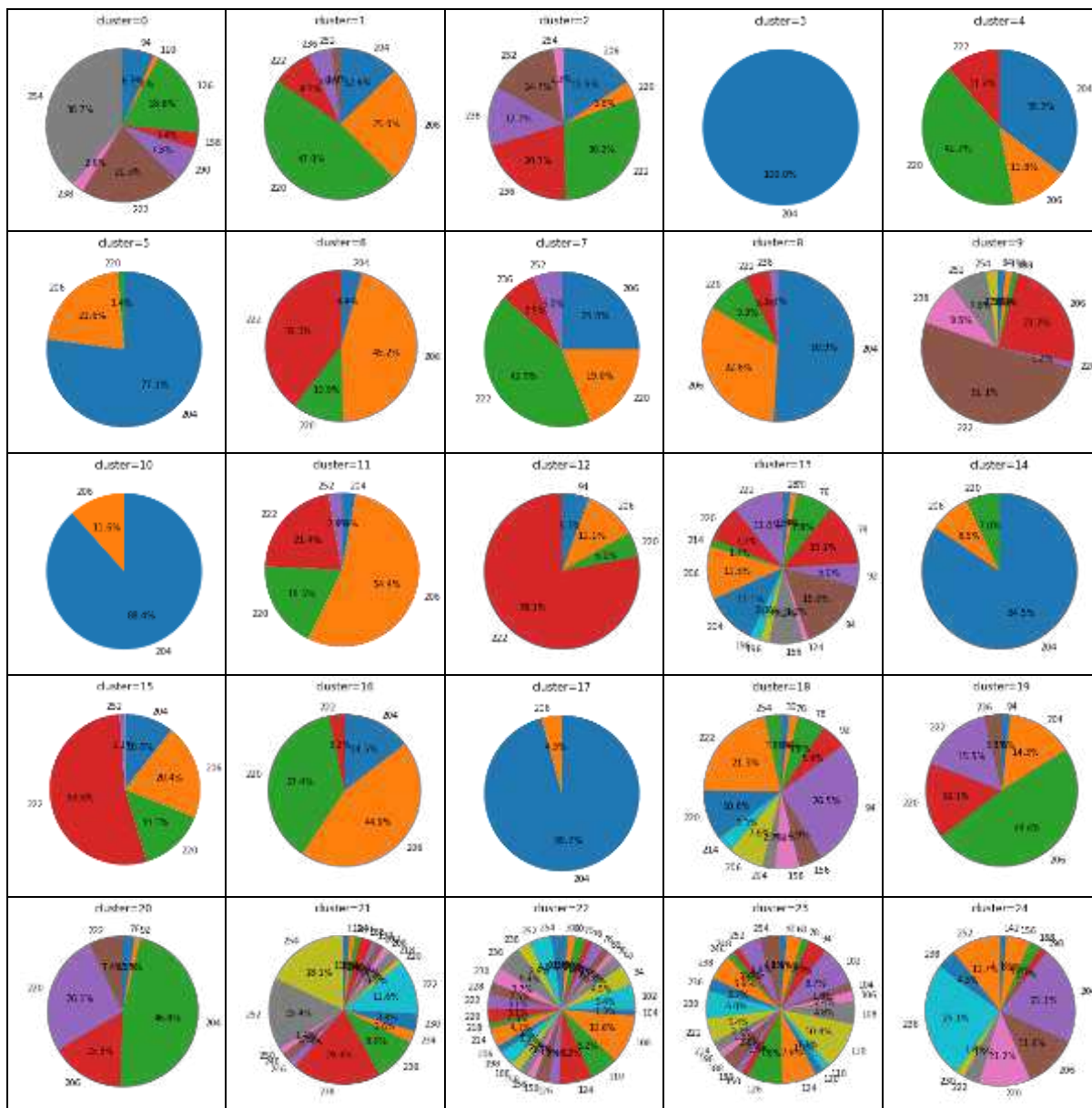
327 **Authors' contributions:** Conceptualization and methodology, G.O., H.S. and H.J.; software and
328 validation, G.O., Y.W., H.K., S.C. and H.J.; formal analysis, investigation and resources, Y.W.,H.K.,
329 Y.K., S.C. and H.J.; writing—original draft preparation, G.O. and H.J.; writing—review and editing,
330 Y.K., Y.W. and H.J.; visualization, G.O. and H.J.; supervision, H.S. and H.J.; funding acquisition, H.S.
331 and H.J.

332 **Correspondence and requests for materials should be addressed to H.J.**

333 **Data Availability** All data generated or analysed during this study are included in this published article.

334 **A Percentile Distribution of probabilities of predicted rules for 25 clusters**

335 The trained CNN gives us the rule distribution for 25 clusters. In fact, the CNN provides a percentile
 336 distribution for 128 rules, of which only those that occur more than 1% are shown in the circle diagram.
 337



338 **Figure 8.** Percentile Distribution of predicted rules by cluster. It shows percentile distribution of the rules for
 339 25 clusters. It is obtained by learning ECA rules to each cluster. The percentile distribution of the rules is obtained
 340 using the trained parameters of CNN.

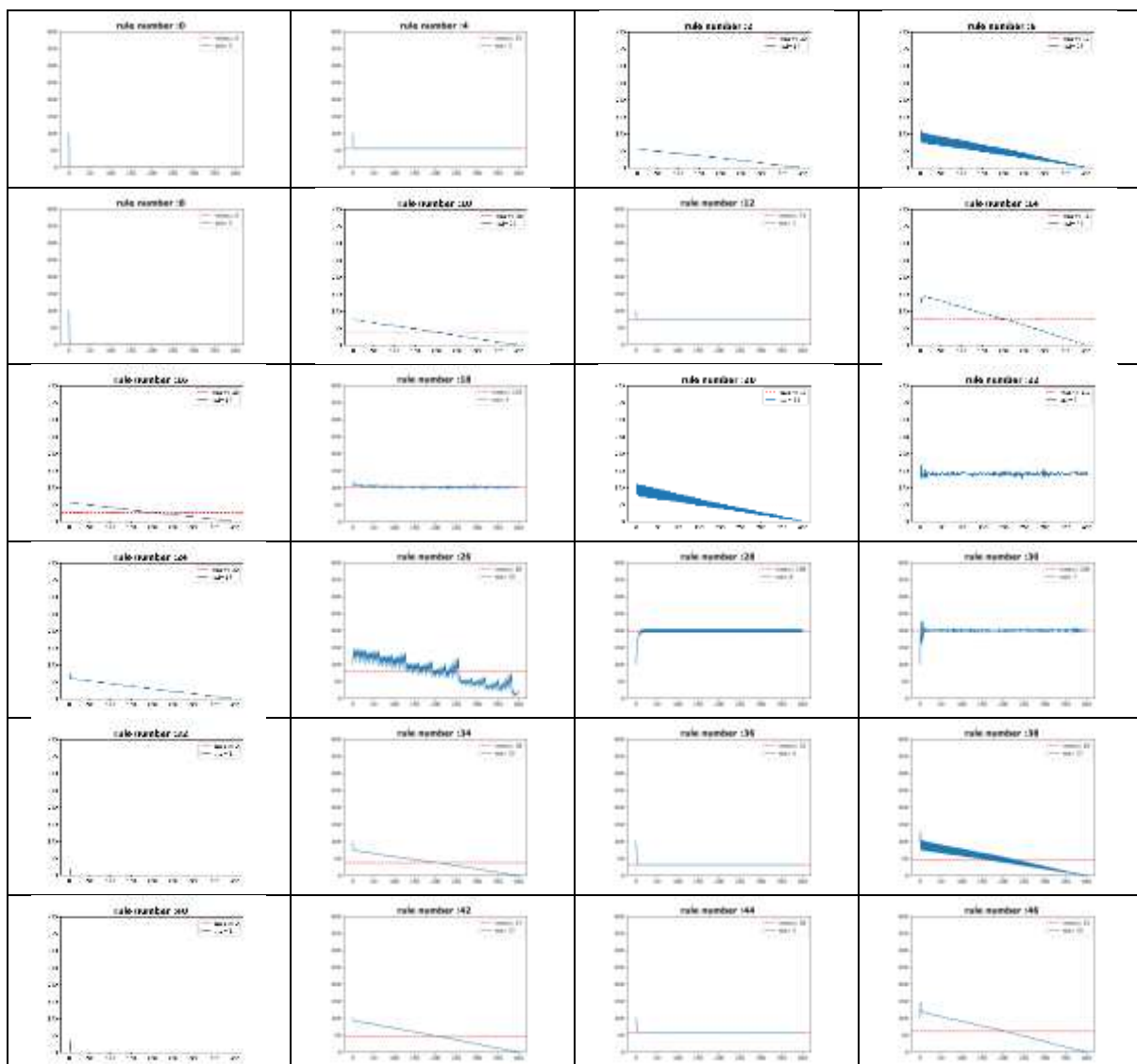
341

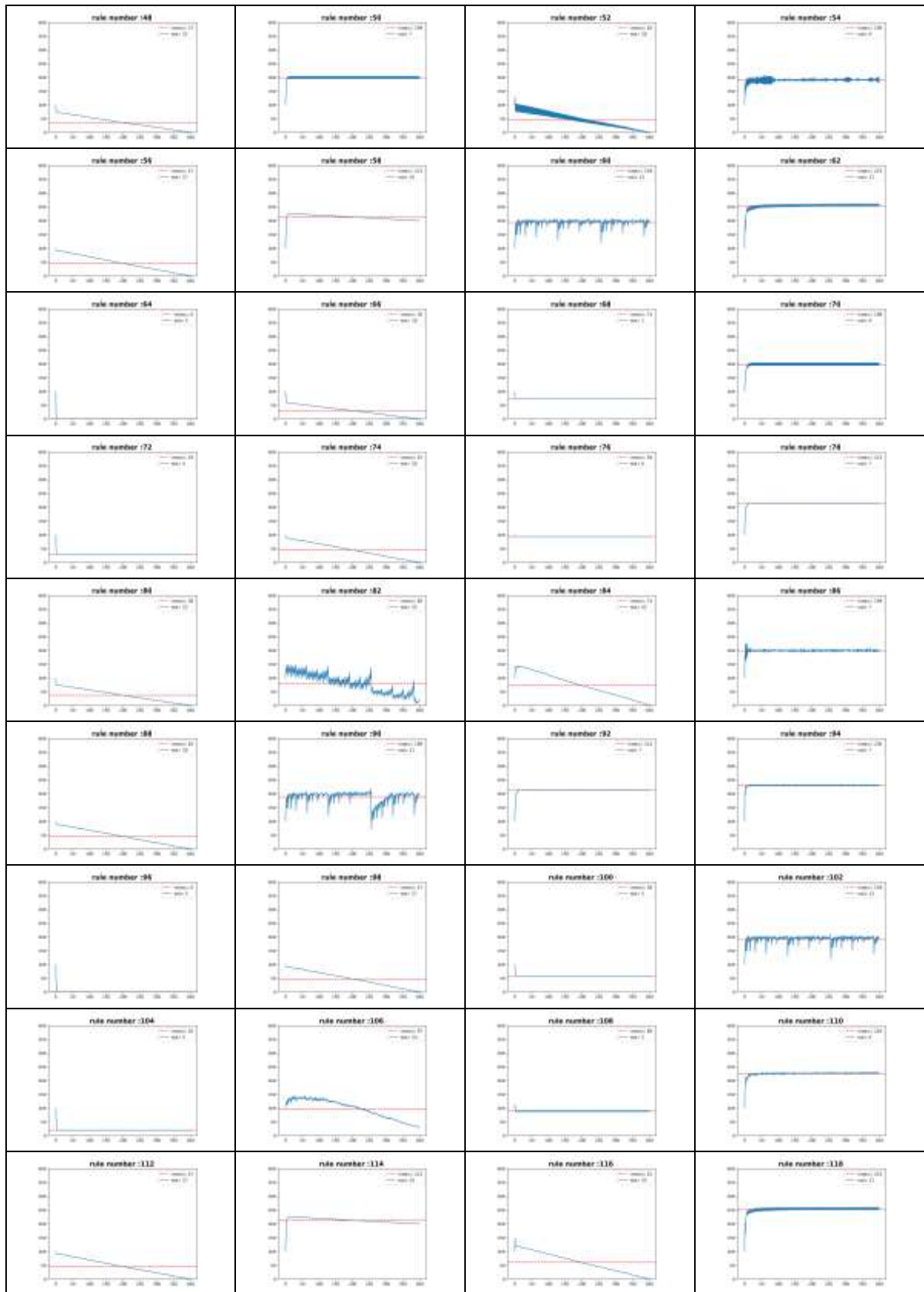
342 **B Variation patterns of even ECA rules.**

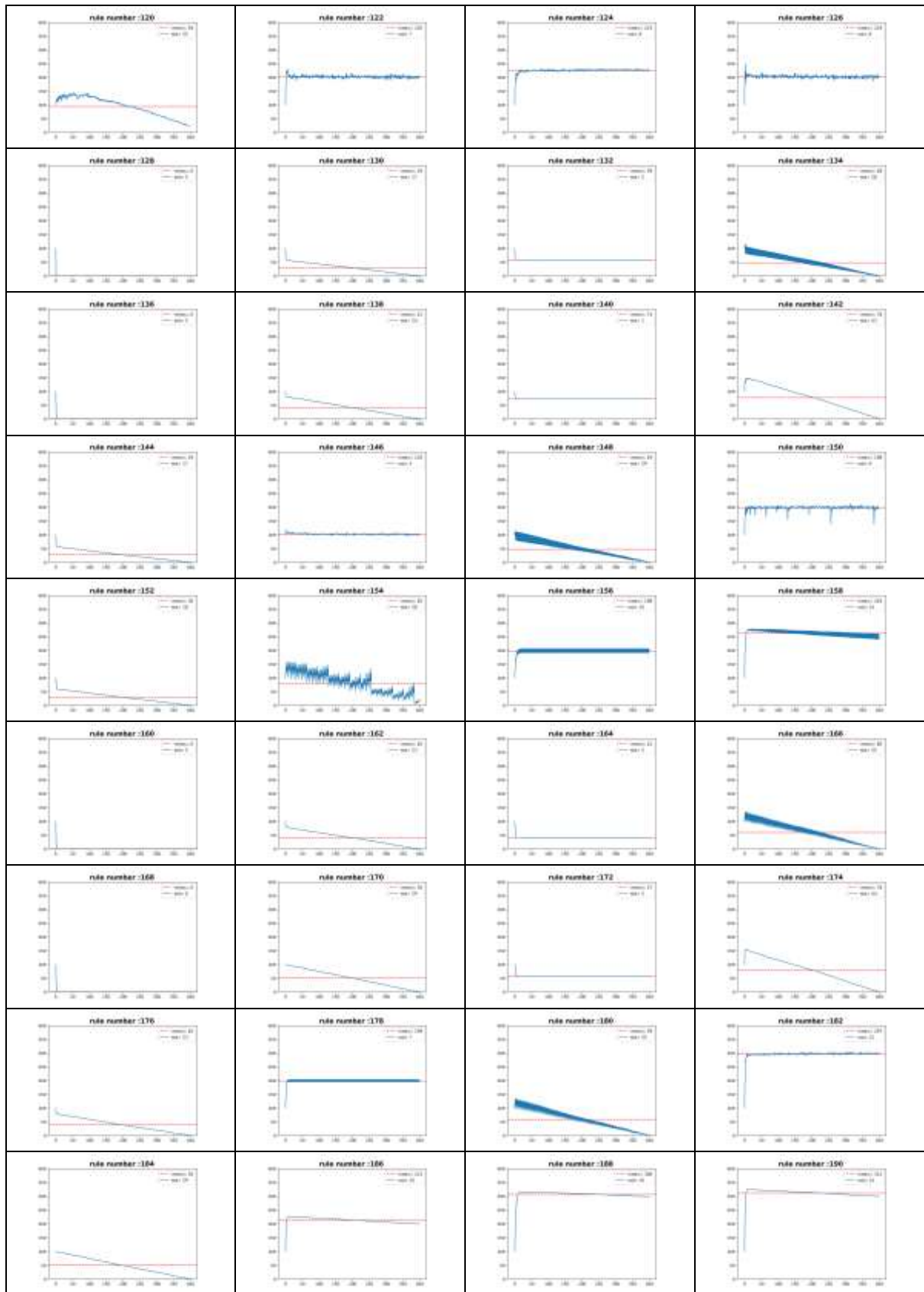
343 A value of 1 is randomly assigned to 100 cells out of 400 cells, and the number of cells having a value
 344 of 1 is counted up to 400 generations according to ECA rules. This process is repeated 10 times and the
 345 average value is obtained. Cells with a value of 1 correspond to the Bullfrog Observed Sites (BOS).
 346 The mean value is shown as a red dotted line, and according to the rules, the number of estimated BOS
 347 either maintains the mean value line, decreases, or shows various types of oscillations around the line.

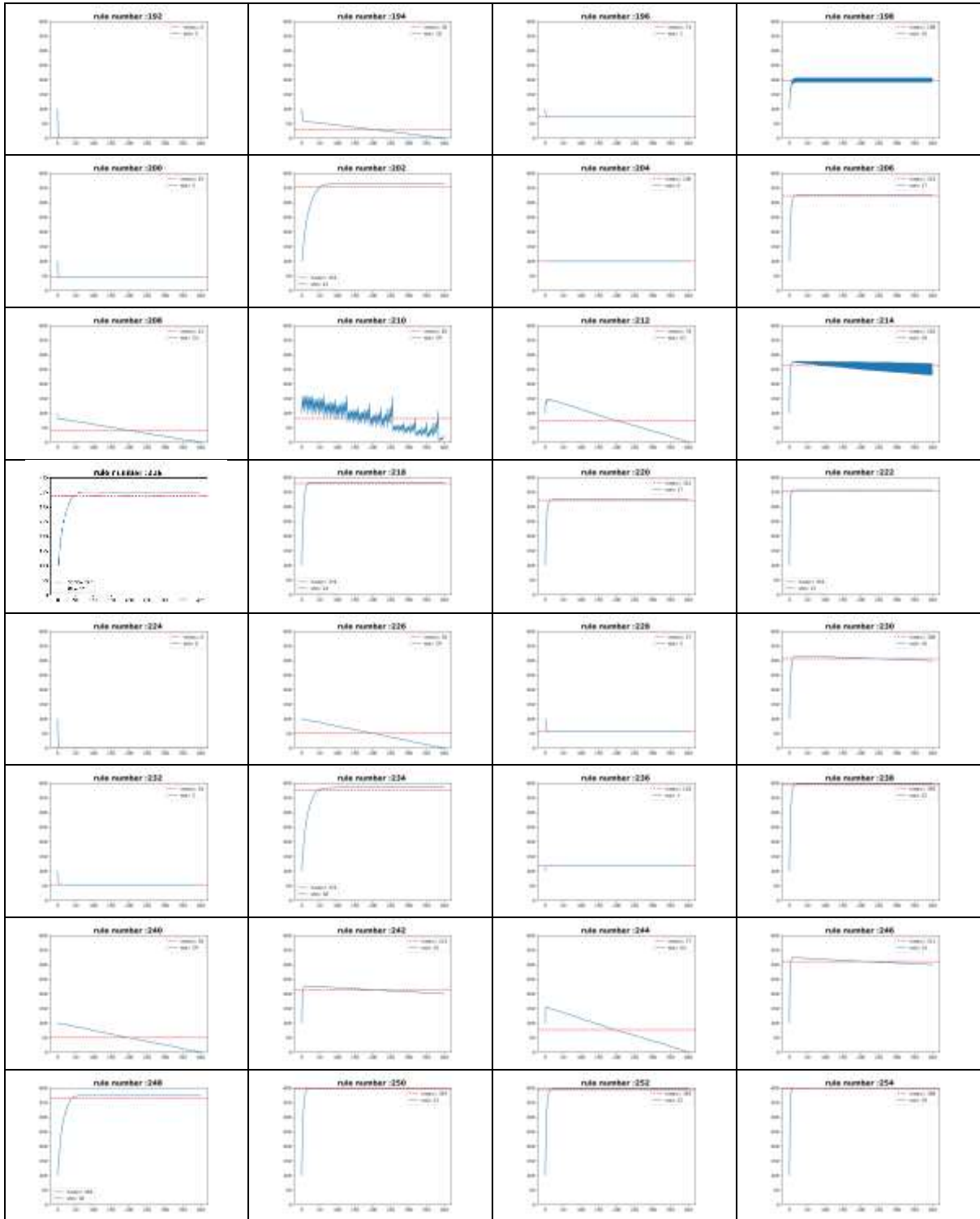
348

349 **Table 3.** Variations in the expected number of BOS over 400 generations according to the ECA even
 350 number rules.









351
352

353 **Reference**

354

355 Brodrick Philip G, Davies Andrew B, Asner Gregory P (2019) Uncovering ecological patterns with
356 convolutional neural networks. *Trends in ecology & evolution* 34(8): 734-745.

357 <https://doi.org/10.1016/j.tree.2019.03.006>

358 Chang Byungwoo, Kim Inyoo, Choi Kwanghun, Cho Wonhee, Ko Dongwook W (2022) Population
359 Dynamics of American Bullfrog (*Lithobates catesbeianus*) and Implications for Control.
360 *Animals* 12(20): 2827.

361 da Silveira Vasconcelos Tiago, Rodríguez Miguel Ángel, Hawkins Bradford Alan (2011) Biogeographic
362 distribution patterns of South American amphibians: a regionalization based on cluster
363 analysis. *Journal of Biogeography* 39: 1720-1732. <https://doi.org/10.4322/natcon.2011.008>

364 Database Global Invasive Species (2023) Global Invasive Species Database.
365 http://www.iucngisd.org/gisd/100_worst.php. Accessed 28 Mar 2023

366 Deneu Benjamin, Servajean Maximilien, Bonnet Pierre, Botella Christophe, Munoz François, Joly
367 Alexis (2021) Convolutional neural networks improve species distribution modelling by
368 capturing the spatial structure of the environment. *PLoS computational biology* 17(4):
369 e1008856. <https://doi.org/10.1371/journal.pcbi.1008856>

370 Duryea Jack (2018) Cellular Automata and Their Elegant Complexities: Musings about Blockchain,
371 Quantum Computing, and AI. *Medium* HackerNoon.com.
372 [https://medium.com/hackernoon/cellular-automata-and-their-elegant-complexities-](https://medium.com/hackernoon/cellular-automata-and-their-elegant-complexities-musings-about-blockchain-quantum-computing-and-c8d2c2d1cf70)
373 [musings-about-blockchain-quantum-computing-and-c8d2c2d1cf70](https://medium.com/hackernoon/cellular-automata-and-their-elegant-complexities-musings-about-blockchain-quantum-computing-and-c8d2c2d1cf70). Accessed 15 Jul 2007

374 Elith* Jane, H. Graham* Catherine, P. Anderson Robert, Dudík Miroslav, Ferrier Simon, Guisan Antoine,
375 et al. (2006) Novel methods improve prediction of species' distributions from occurrence
376 data. *Ecography* 29(2): 129-151. <https://doi.org/10.1111/j.2006.0906-7590.04596.x>

377 Ermentrout G Bard, Edelstein-Keshet Leah (1993) Cellular automata approaches to biological
378 modeling. *Journal of theoretical biology* 160(1): 97-133.
379 <https://doi.org/10.1006/jtbi.1993.1007>

380 Ficetola Gentile Francesco, Maiorano Luigi, Falcucci Alessandra, Dendoncker Nicolas, Boitani Luigi,
381 PADOA-SCHIOPPA EMILIO, et al. (2010) Knowing the past to predict the future: land-use
382 change and the distribution of invasive bullfrogs. *Global change biology* 16(2): 528-537.
383 <https://doi.org/10.1111/j.1365-2486.2009.01957.x>

384 Ficetola Gentile Francesco, Thuiller Wilfried, Miaud Claude (2007) Prediction and validation of the
385 potential global distribution of a problematic alien invasive species—the American bullfrog.
386 *Diversity and distributions* 13(4): 476-485. <https://doi.org/10.1111/j.1472-4642.2007.00377.x>

387 Giovanelli Joao GR, Haddad Célio FB, Alexandrino Joao (2008) Predicting the potential distribution
388 of the alien invasive American bullfrog (*Lithobates catesbeianus*) in Brazil. *Biological*
389 *Invasions* 10: 585-590. <https://doi.org/10.1007/s10530-007-9154-5>

390 Groffen Jordy, Kong Sungsik, Jang Yikweon, Borzée Amaël (2019) The invasive American bullfrog
391 (Lithobates catesbeianus) in the Republic of Korea: history and recommendations for
392 population control. *Management of Biological Invasions* 10(3): 517.
393 <http://dx.doi.org/10.3391/mbi.2019.10.3.08>

394 Harris Charles R, Millman K Jarrod, Van Der Walt Stéfán J, Gommers Ralf, Virtanen Pauli, Cournapeau
395 David, et al. (2020) Array programming with NumPy. *nature* 585(7825): 357-362.

396 Iñiguez Carlos A, Morejón Felipe J (2012) Potential distribution of the American bullfrog (Lithobates
397 catesbeianus) in Ecuador. *south american Journal of herpetology* 7(2): 85-90.
398 <https://doi.org/10.2994/057.007.0211>

399 Jang HJ, Suh JH (2010) Distribution of amphibian species in South Korea. *Korean Journal of*
400 *Herpetology* 2: 45-51.

401 Kamaroff Colleen, Daniele Ninette, Grasso Robert L, Rising Rebecca, Espinoza Travis, Goldberg Caren
402 S (2020) Effective removal of the American bullfrog (Lithobates catesbeianus) on a landscape
403 level: long term monitoring and removal efforts in Yosemite Valley, Yosemite National Park.
404 *Biological Invasions* 22(2): 617-626. <https://doi.org/10.1007/s10530-019-02116-4>

405 Kang Hee-Jin, Koo Kyo Soung, Sung Ha-Cheol (2019) Current distribution of American bullfrog *Rana*
406 *catesbeiana* Shaw, 1802 in the Republic of Korea. *BioInvasions Records* 8(4): 942-946.
407 <https://doi.org/10.3391/bir.2019.8.4.23>

408 Kattenborn Teja, Leitloff Jens, Schiefer Felix, Hinz Stefan (2021) Review on Convolutional Neural
409 Networks (CNN) in vegetation remote sensing. *ISPRS journal of photogrammetry and*
410 *remote sensing* 173: 24-49. <https://doi.org/10.1016/j.isprsjprs.2020.12.010>

411 Kim JB (2009) Taxonomic list and distribution of Korean amphibians. *Korean J. Herpetol* 1: 1-13.

412 Koo Kyo Soung, Choe Minjee (2021) Distribution Change of Invasive American Bullfrogs (Lithobates
413 catesbeianus) by Future Climate Threaten Endangered Suweon Treefrog (Hyla suweonensis)
414 in South Korea. *Animals* 11(10): 2865. <https://doi.org/10.3390/ani11102865>

415 LeCun Yann, Bengio Yoshua, Hinton Geoffrey (2015) Deep learning. *nature* 521(7553): 436-444.
416 <https://doi.org/10.1038/nature14539>

417 Martín Abadi, Ashish Agarwal, Paul Barham, Eugene Brevdo, Zhifeng Chen, Craig Citro, et al. (2015)
418 TensorFlow: Large-Scale Machine Learning on Heterogeneous Systems.
419 <https://www.tensorflow.org/>. Accessed

420 Martínez Genaro J, Adamatzky Andrew, Alonso-Sanz Ramon (2012) Complex dynamics of elementary
421 cellular automata emerging from chaotic rules. *International Journal of Bifurcation and*
422 *Chaos* 22(02): 1250023. <https://doi.org/10.1142/S021812741250023X>

423 Nagatani Takashi, Tainaka Kei-ichi (2018) Cellular automaton for migration in ecosystem: Application
424 of traffic model to a predator-prey system. *Physica A: Statistical Mechanics and its*
425 *Applications* 490: 803-807. <https://doi.org/10.1016/j.physa.2017.08.151>

426 No Sun-Ho, Jung Jin-Seok, You Young-Han (2017) Ecological control of invasive alien species,

427 American bullfrog (*Rana catesbeiana*) using native predatory species. *Korean Journal of*
428 *Environment and Ecology* 31(1): 54-61. <https://doi.org/10.13047/KJEE.2017.31.1.054>

429 Nori Javier, Urbina-Cardona J Nicolás, Loyola Rafael D, Lescano Julian N, Leynaud Gerardo C (2011)
430 Climate change and American bullfrog invasion: what could we expect in South America?
431 *PloS one* 6(10): e25718. <https://doi.org/10.1371/journal.pone.0025718>

432 Oh Hong-Shik, Hong Chang-Eui (2007) Current conditions of habitat for *Rana catesbeiana* and
433 *Trachemys scripta elegans* imported to Jeju-do, including proposed management plans.
434 *Korean Journal of Environment and Ecology* 21(4): 311-317.

435 Park Hye-Rin, Rahman Md Mizanur, Park Seung-Min, Choi Jae-Hyeok, Kang Hee-Jin, Sung Ha-Cheol
436 (2022) Risk assessment for the native anurans from an alien invasive species, American
437 bullfrogs (*Lithobates catesbeianus*), in South Korea. *Scientific reports* 12(1): 13143.
438 <https://doi.org/10.1038/s41598-022-17226-8>

439 Patlolla Chaitanya Reddy. (2018). Understanding the concept of Hierarchical clustering Technique.
440 Retrieved from Medium website: [https://towardsdatascience.com/understanding-the-](https://towardsdatascience.com/understanding-the-concept-of-hierarchical-clustering-technique-c6e8243758ec)
441 [concept-of-hierarchical-clustering-technique-c6e8243758ec](https://towardsdatascience.com/understanding-the-concept-of-hierarchical-clustering-technique-c6e8243758ec)

442 Pedregosa Fabian, Varoquaux Gaël, Gramfort Alexandre, Michel Vincent, Thirion Bertrand, Grisel
443 Olivier, et al. (2011) Scikit-learn: Machine learning in Python. *the Journal of machine Learning*
444 *research* 12: 2825-2830.

445 Phillips Steven J, Anderson Robert P, Dudík Miroslav, Schapire Robert E, Blair Mary E (2017) Opening
446 the black box: An open-source release of Maxent. *Ecography* 40(7): 887-893.
447 <https://doi.org/10.1111/ecog.03049>

448 Phillips Steven J, Anderson Robert P, Schapire Robert E (2006) Maximum entropy modeling of species
449 geographic distributions. *Ecological modelling* 190(3-4): 231-259.
450 <https://doi.org/10.1016/j.ecolmodel.2005.03.026>

451 Phillips Steven J, Dudík Miroslav (2008) Modeling of species distributions with Maxent: new
452 extensions and a comprehensive evaluation. *Ecography* 31(2): 161-175.
453 <https://doi.org/10.1111/j.0906-7590.2008.5203.x>

454 Phillips Steven J. (2017) A Brief Tutorial on Maxent.
455 http://biodiversityinformatics.amnh.org/open_source/maxent/. Accessed 14 Aug 2023

456 Qin Jiaohua, Pan Wenyan, Xiang Xuyu, Tan Yun, Hou Guimin (2020) A biological image classification
457 method based on improved CNN. *Ecological Informatics* 58: 101093.
458 <https://doi.org/10.1016/j.ecoinf.2020.101093>

459 Schlaepfer Martin A, Sherman Paul W, Blossey Bernd, Runge Michael C (2005) Introduced species
460 as evolutionary traps. *Ecology Letters* 8(3): 241-246. [https://doi.org/10.1111/j.1461-](https://doi.org/10.1111/j.1461-0248.2005.00730.x)
461 [0248.2005.00730.x](https://doi.org/10.1111/j.1461-0248.2005.00730.x)

462 Tesfamariam Birhane Gebrehiwot, Gessesse Berhan, Melgani Farid (2022) MaxEnt-based modeling of
463 suitable habitat for rehabilitation of *Podocarpus* forest at landscape-scale. *Environmental*

464 Systems Research 11(1): 1-12. <https://doi.org/10.1186/s40068-022-00248-6>
465 Venne Simon, Currie David J (2021) Can habitat suitability estimated from MaxEnt predict
466 colonizations and extinctions? Diversity and distributions 27(5): 873-886.
467 <https://doi.org/10.1111/ddi.13238>
468 Webb Sarah (2018) Deep learning for biology. nature 554(7693): 555-557.
469 <https://doi.org/10.1038/d41586-018-02174-z>
470 Weisstein Eric W (2017) Elementary Cellular Automaton. MathWorld--A Wolfram Web Resource.
471 <https://mathworld.wolfram.com/ElementaryCellularAutomaton.html>. Accessed
472 Wolfram Stephen (1983) Statistical mechanics of cellular automata. Reviews of modern physics 55(3):
473 601. <https://doi.org/10.1103/RevModPhys.55.601>
474 Wolfram Stephen (2002) *A new kind of science* (Vol. 5). Wolfram media Champaign, IL.
475